Estimating Alertness from the EEG Power Spectrum

Tzyy-Ping Jung, Scott Makeig, Magnus Stensmo, and Terrence J. Sejnowski

Abstract

In tasks requiring sustained attention, human alertness varies on a minute time scale. This can have serious consequences in occupations ranging from air traffic control to monitoring of nuclear power plants. Changes in the electroencephalographic (EEG) power spectrum accompany these fluctuations in the level of alertness, as assessed by measuring simultaneous changes in EEG and performance on an auditory monitoring task. By combining power spectrum estimation, principal component analysis and artificial neural networks, we show that continuous, accurate, noninvasive, and near real-time estimation of an operator's global level of alertness is feasible using EEG measures recorded from as few as two central scalp sites. This demonstration could lead to a practical system for noninvasive monitoring of the cognitive state of human operators in attention-critical settings.

Keywords

EEG; power spectrum; alertness; neural networks; vigilance; neural human-system interfaces

I. INTRODUCTION

Many studies of vigilance during the past half century have shown that retaining a constant level of alertness is difficult or impossible for operators of automatized systems who perform monotonous but attention-demanding monitoring tasks [1]. Alertness deficits are a particular problem in around-the-clock operations, and can lead to severe consequences for ship, air, truck, rail, or plant operators, air traffic controllers, security officers, and workers in many other occupations. In most such work environments, continuous measures of operator performance are not available. Accurate and non-intrusive real-time monitoring of operator alertness would thus be highly desirable in a variety of operational environments, particularly if this measure could be shown to predict changes in operator performance capacity.

It has also been known for more than half a century that signal changes related to alertness, arousal, sleep, and cognition are present in electroencephalographic (EEG) recordings [2], [3], [4], [5], but relatively little has been done to capture this information in real time. Our research investigates the feasibility of using multichannel electroencephalographic data to estimate, continuously, accurately, noninvasively, and in near-real time, fluctuations in an operator's global level of alertness.

While most past vigilance research has focused on measuring group mean performance trends, individual performance on monitoring tasks tends to fluctuate irregularly, including periods from two seconds to many minutes of intermittent or complete unresponsiveness [6], [7], [8], [9]. Unfortunately, most vigilance experiments designed to simulate actual work environments have used target presentation rates too low to accurately observe sub-minute-scale performance dynamics. Our research focuses

T-P Jung is with the Computational Neurobiology Laboratory, The Salk Institute, San Diego, CA 92186-5800 and the National Research Council, National Academy of Sciences, Washington, D.C. 20418.

Scott Makeig is with the Cognitive Performance and Psychophysiology Department, Naval Health Research Center, San Diego, CA 92186-5122 and the Department of Neurosciences, University of California, San Diego, La Jolla, CA 92093.

M. Stensmo was with the Computational Neurobiology Laboratory, The Salk Institute, San Diego, CA 92186-5800. He is now with the Department of Computer Science, University of California, Berkeley, Berkeley, CA 94720-1776.

T.J. Sejnowski is with the Computational Neurobiology Laboratory, The Salk Institute, San Diego, CA 92186-5800 and the Department of Biology, University of California, San Diego, La Jolla, CA 92093.

This research was supported by the Department of the Navy, Naval Research and Development Command, Bethesda, Maryland under *ONR.WR.30020(6429)* to Dr. Makeig and *ONR N00014-91-J-1674* to Dr. Sejnowski. The views expressed in this paper are those of the authors and do not reflect the official policy or position of the Department of the Navy, Department of Defense, or the U.S. Government. Approved for release, distribution unlimited.

on continuous changes in human performance and the EEG power spectrum on minute time scales by using an event rate high enough (10/min) to track minute-scale changes in performance. Note that in most complex real-world work environments (especially those involving low-arousal monitoring tasks), detailed knowledge of minute-scale changes in operator performance is not available. In such environments, an EEG-based alertness monitoring system could estimate operators' performance without requiring continuous performance assessment.

Most previous psychophysiological studies of alertness [10], [11], [12] have attempted to use the same estimator for all subjects. However, the relatively large individual variability in EEG dynamics accompanying loss of alertness means that, for many operators, group statistics cannot be used to accurately predict changes in alertness and performance. In contrast, Makeig and Inlow [9] used individualized multiple linear regression models to estimate operators' changing levels of alertness while they performed a laboratory simulation of a passive sonar detection task. The discriminative power and flexibility of neural networks make them good candidates to complement more traditional methods for detecting and modeling the relationship between alertness and the EEG power spectrum. Subsequent analysis showed that artificial neural network models can estimate alertness more efficiently than linear models [13], and this approach was used to construct and test a laboratory model of a real-time alertness monitoring system [14]. Like other studies of the relationship between EEG spectra and performance, however, these studies used the same pre-selected frequency bands for all subjects, resulting in estimators that were partly insensitive to individual frequency-band differences.

In this study, we assess the information on alertness available in each operator's full EEG spectrum. Next, we use this information to develop, for each operator, a neural network estimator using principal component analysis to adapt to individual differences in EEG dynamics accompanying loss of alertness. We then compare the accuracy of our estimates to those obtained from linear regression models. Finally, we present a benchmark study in which the accuracy of our alertness estimates compares favorably to non-EEG based *a priori* models, and show that our estimation results approach a lower bound for error rate estimation.

II. METHODS

A. Subjects

A total of fifteen subjects (ages from 18 to 34 years) participated in a dual-task simulation of auditory and visual sonar target detection. All had passed standard Navy hearing tests or reported having normal hearing. Each subject participated in three or more simulated work sessions each lasting 28 minutes. We selected for intensive analysis data from all subjects having at least two sessions containing a minimum of 25 lapses. For each of these (10) subjects, we selected the two sessions with the highest number of lapses for training and testing, and reserved the session with the third highest number of lapses for neural network training validation. The twenty selected test sessions included a mean of 68 lapses (range: 27-160).

B. Stimuli

Auditory signals, including background noise, tone pips, and noise burst targets, were synthesized using a Concurrent work station which was also used to record the EEG. In a continuous 63 dB white-noise background, task-irrelevant auditory tones at two frequencies (568 Hz and 1098 Hz) were presented in random order at 72 dB (normal hearing level) with stimulus onset asynchronies between 2-4 s. These signals were introduced to assess the information available in event-related potentials [13], and are not reported in this study. In half of the inter-tone intervals, target noise bursts were presented at 6 dB above their detection threshold. The mean target rate was thus 10 per minute. Positions of target onsets in the inter-tone intervals were pseudorandom, and did not occur within 400 ms of the nearest probe tone.

Visual stimuli were produced by a 386 PC with a VGA color display (13-cm wide by 9-cm high). The display background was composed of 1-mm grey scale squares resembling visual television noise ("snow"). Visual targets were introduced at a mean rate of 1 per min, and were not correlated with auditory targets. Visual targets consisted of 20 consecutive white squares forming a vertical line. The display was updated twice each second by adding a new line of squares to the top of the screen and scrolling the existing display down one line, creating a slowly descending "waterfall" effect.

C. Procedure

Each subject participated in three or more 28-min experimental sessions on separate days. Subjects sat in a chair with their right index and middle fingers resting on visual and auditory target response buttons, respectively. The subjects viewed the CRT waterfall display while receiving auditory stimulation bilaterally through headphones, and pressed the auditory or visual response buttons each time they detected an auditory or visual target respectively.

D. Data Collection

EEG data were recorded at a sampling rate of 312.5 Hz from two midline sites, one central (Cz) and the other midway between parietal and occipital sites (Pz/Oz), using 10-mm gold-plated electrodes referenced to the right earlobe. EEG data were first preprocessed using a simple out-of-bounds test (with a +/-50 uV threshold) to reject epochs that were grossly contaminated by muscle and/or eye-movement artifacts. Moving-averaged spectral analysis of the EEG data was then accomplished using a 256-point Hanning-window with 50% overlap. Windowed 256-point epochs were extended to 512 points by zero-padding. Median filtering using a moving 5-s window was used to further minimize the presence of artifacts in the EEG records. The EEG power spectrum time series for each session consisted of 1024 EEG power estimates at 81 frequencies (from 0.61 to 49.41 Hz) at 1.6384-s (512-point, an epoch) time intervals. For spectral correlation and error rate estimation, data from each session were first converted to a logarithmic scale and then normalized at each frequency separately by subtracting the session mean and dividing the result by half the difference between the 25th and 75th percentiles of the log power distribution during the session. Logarithmic scaling linearizes the expected multiplicative effects of subcortical systems involved in wake-sleep regulation on EEG amplitudes [15].

E. Alertness Measure

Auditory targets were classified as Hits or Lapses depending on whether or not the subject pressed the auditory response button within 120 ms to 3000 ms of target onset. To quantify the level of alertness, auditory responses were converted into *local error rate*, defined as the fraction of targets not detected by the subject (i.e. lapses) within a moving time window. Each error rate time series consisted of 1024 points at 1.6384 s intervals, and was computed using a causal 93.4 s (57 epoch) exponential window whose gain varied from 1.0 at the leading edge to 0.1 at the trailing edge. Error rate and EEG data from the first 93.4 s of each run were not used in the analysis. For each window position, the sum of window values at moments of presentation of undetected (lapse) targets was divided by the sum of window values at moments of presentation of all targets. The window was moved through the session in 1.6-s steps, converting the irregularly-sampled, discontinuous performance record into a regularly-sampled, continuous error rate measure with range [0,1].

F. Numerical Methods

Numerical results in this study were computed on a Silicon Graphics Indy computer (R4000PC CPU). The stability of minute-scale fluctuations in performance concurrent with changes in the EEG power spectrum over time and subjects was analyzed using a cluster analysis program, Unix *pca/cluster*, based on the centroid method [16]. Multivariate linear regression and analysis of variance were performed using Unix/stat, a set of data-manipulation an data-analysis programs [17].

Analysis using feedforward multi-layer perceptrons was performed using the *Xerion* neural network simulator [18]. A feedforward multi-layer perceptron network has an input layer, an output layer, and often one or more intermediate or hidden layers. Nodes in successive layers are connected by continuously adjustable parameters or weights. Each node computes a weighted sum of its inputs, which is then passed through a nonlinear monotonic squashing function. In this study, the weights and biases of the network were adjusted using the error back-propagation algorithm [19]. The conjugate gradient descent method was used to minimize sum-squared error between the network and desired outputs for the 967 time points (the whole session excluding the first 57 epochs) from the training session. Cross validation [20] using 967 time points from the reserved third session from the same subject was applied to prevent the network from overfitting the training data. Training was terminated when estimation performance on validation data ceased to improve. Upon completion of the training, which typically took several minutes of CPU time, the network was tested on the last 967 data points from a separate session for the same subject. We then repeated this procedure with the roles of training and testing sessions reversed in order to evaluate the estimation performance on a larger quantity of training-testing pairs. Estimation performance of different models was compared using analysis of variance of root mean square (rms) estimation errors during each run (excluding the first 93.4 s).

III. RELATIONSHIP BETWEEN THE EEG SPECTRUM AND ALERTNESS

Figure 1 shows changes in the log EEG spectrum at the vertex accompanying changes in local error rate during a typical session. In the figure, the EEG log spectrum has been normalized by subtracting the mean log spectrum during the first 2 minutes of the session, during which the subject made no errors. Note the apparent correlation between increased local error rate and EEG power below 5 Hz, and the sharp increases in power near 14 Hz (the human 'sleep-spindling' frequency) during two peak error rate periods (minutes 18 and 28).

[Figure 1 about here.]

A. Error-sorted EEG spectra

To investigate the relationship of minute-scale fluctuations in performance to concurrent changes in the EEG spectrum, we first computed mean power spectra for "alert" (0% error rate) epochs in each session, then computed ratios between the spectrum at each time point and the mean "alert" spectrum for that session. We then sorted the spectral ratios by local error rate, smoothed the sorted data using a bell-shaped Papoulis window [21] (base width: 30% error-rate), which was advanced through the sorted spectral differences in small steps (2% error-rate), and averaged the resulting surfaces across the 20 test sessions.

[Figure 2 about here.]

Figure 2(a) shows the resulting grand mean normalized *error-sorted spectrum* at Cz for the 10 subjects. Depth indexes local error rate, with greater depth corresponding to higher error rate. The horizontal axis indexes EEG frequency. Figure 2(b) shows the resulting error-sorted spectrum at Pz/Oz. Several features are noteworthy. First, at Cz there is strong evidence of a monotonic relationship between fluctuations in EEG power and performance in two relatively narrow bands, near 3.7 Hz and 14.7 Hz. In both bands, as local error rate increases, so does the EEG power, i.e. fluctuations in EEG power are positively correlated with fluctuations in local error rate. Second, at Pz/Oz a similar monotonic relationship exists between the fluctuations in EEG power and performance in a wider frequency band around 4 Hz, but the peak near 14 Hz is less prominent and appears only when error rate exceeds 75%. Third, at Cz, power near 4 Hz does not increase appreciably, relative to baseline, when error rate is under 50%, while at Pz/Oz, the relationship between fluctuations in EEG power and performance is more monotonic throughout the local error rate range (cross-section plots of Fig. 2). Fourth, near 10 Hz the error-sorted spectral surfaces at low error rates are relatively flat, in contrast to previous

results on subjects performing a similar auditory task with eyes closed [9]. This suggests that alpha frequencies (8-12 Hz) may be of relatively little use for error rate estimation in subjects whose eyes are open. Note that evoked responses to the visual and auditory stimuli used in the experiment could contribute very little to the EEG spectrum and spectral correlations, since normal evoked response activity is much weaker than the spontaneous EEG activity it accompanies. Fluctuations in visual task performance, which were generally correlated with auditory task performance changes, will be reported elsewhere.

B. Spectral Correlation

We then measured correlations between changes in the EEG log power spectrum and local error rate by computing the correlations between the two time series at each EEG frequency. We refer to the results as forming a *correlation spectrum*. Since most spectral variance in the error rate time series for this task occurs at cycle lengths longer than 4 minutes [9], we smoothed the EEG power and error rate time series using a non-causal 93.4-s bell-shaped moving-average filter to eliminate variance at cycle lengths shorter than 1-2 minutes. For each EEG site and frequency, we then computed spectral correlations for each session separately and averaged the results across all 20 sessions. Results for 40 frequencies between 0.61 Hz and 24.4 Hz are shown in Fig. 3(a).

[Figure 3 about here.]

As suggested by the peaks in the error-sorted spectral surfaces (Figure 2), the mean correlation between performance and EEG power is positive at both sites near 4 Hz, and at Cz another positive correlation occurs near 14 Hz. At high error rates, a modest negative correlation also appears near 10 Hz. In an earlier study using the same auditory detection task, where subjects kept their eyes closed [9], the spectral correlation between performance and EEG power contained a prominent negative correlation in the alpha frequency range. This negative peak was not found in the present experiments in which subjects performed with eyes open. Figure 3(a) gives the impression that two frequency bands dominate the relationship between performance and the EEG power spectrum.

Next, we compared correlation spectra for individual sessions to examine the stability of this relationship over time and subjects. Figure 3(b),(c), and (d) show that correlation spectra for three subjects are consistent between sessions, but differ between subjects. Subject D3 shows a positive correlation between error rate and log power at 14 Hz, while subject D2 does not. Cluster analysis of spectral correlations between EEG and error rates for all 20 sessions from the 10 subjects (Figure 4) shows that pairs of sessions from each subject were clustered either adjacent to or near to one another. Even the pair of sessions most widely separated by the cluster analysis (D14) share a moderate positive correlation between 1 Hz and 10 Hz at both scalp locations (Figure 3(d)). Thus, changes in the EEG spectrum accompanying loss of alertness appear to be stable within, but somewhat variable between subjects.

[Figure 4 about here.]

In summary, the above analyses provide strong and converging evidence that changes in auditory detection performance during a sustained attention task are monotonically related to changes in the EEG power spectrum at several frequencies. This relationship is relatively variable between subjects, but stable within subjects. These findings suggest that information available in the EEG can be used for real-time estimation of changes in alertness of human operators performing monitoring tasks. However, for maximal accuracy the estimation algorithm should be capable of adapting to individual differences in the mapping between EEG and alertness.

IV. ESTIMATION OF ALERTNESS

An earlier study [9] of alertness estimation based on a similar auditory detection task used linear regression to estimate the time course of local error rate from changes in EEG power at five pre-

set frequencies. However, the individual variability in EEG dynamics accompanying loss of alertness, shown in previous sections, suggests that for many operators, standard narrow frequency bands cannot be used to accurately predict individual changes in alertness and performance. Rather information about alertness may be distributed over the entire EEG spectrum. In this study, we assess the potential accuracy of error rate estimation using full spectrum EEG. First, we describe a lower bound for estimation error and two *a priori* error rate models. Next, we explore the benefits of estimating error rate from the full EEG spectrum at two scalp sites using neural networks. Finally, we compare the results of EEG-based error rate estimation to the lower bound and *a priori* models.

A. Non-EEG Based Estimation

A.1 Estimation Error in *A Priori* Models

The best available *a priori* estimate of local error rate in our task is the group mean local error rate at each instant. The estimate is based on the assumption that for each subject and session the tendency of failing to respond to targets is the same. We computed this "group trend" by averaging performance results of a total of 98 similar 28-minute auditory detection sessions, including the 30 sessions used in the present analysis. The results (Figure 5) follows a well-known trend of vigilance data: Initial near-perfect performance begins to decay after about one minute. Thereafter, error rate rises steadily until 10 min into the task, after which it remains more or less stable near 30%. Thus, this group trend should give a best available *a priori* estimate of alertness decrements. Root mean square errors between the group trend and observed error rate time courses in these experiments thus provide a conservative benchmark for the accuracy of EEG-based alertness estimation. If EEG-based estimation can perform better than this *a priori* estimate, its further development would appear justified. Note that in more complex real-world work environments in which EEG-based monitoring would be of most value, detailed knowledge of the time course of error rates would not normally be available.

A second, less conservative standard can be derived from a model which assumes that operators experience no lapses in alertness at all (a "right stuff" model), ignoring the tendency for vigilance decrements in stimulus-poor environments. Many current system designs may incorporate this model tacitly if they assume that their human operators will be able to respond at any time to new events or conditions. The prediction error of this "right stuff" model, the actual rms error rate for each session, thus provides a second standard against which to compare the performance of EEG-based models.

[Figure 5 about here.]

A.2 Expected Minimum for Estimation Error

Our performance analysis is based on the assumption that the time-varying error-rate measure indexes more or less continuous changes in subjects' levels of alertness. As a probability measure, error rate cannot itself predict individual responses to targets, even if it is known precisely. Since target stimuli in our experiments were delivered at semi-random intervals at a limited sampling rate, the resulting sparse sampling and sampling jitter in the performance records produced uncertainty in error rate estimates computed from those records. In this sense, a local error rate time series cannot be recaptured perfectly from a single performance record. Therefore, any measure partially or wholly correlated with performance, including the EEG spectrum, cannot to be expected to generate an error-rate estimate with more accuracy than is possible in computing local error rate from the performance record.

This reasoning allows us to compute an expected lower bound for error in error-rate estimation. For each session, we first generated 50 surrogate data sessions, series of simulated hits and lapses based on target delivery times generated by the same algorithm that produced the experimental sessions, and counted each target depending on a random number weighted by the observed error rate time series (considered as an experimentally-derived time-varying probability of a performance lapse at each

target delivery time). Next, we low-pass filtered the resulting surrogate performance records using the same smoothing window used to derive the actual error-rate time series. Finally, we computed the rms difference between the resulting surrogate error rate series and the original error rate series for the session. By this method, 50 surrogate error rate functions were created and evaluated for each of the 20 experimental sessions. Figure 6 shows the error rate time series from one session (top panel) and 20 surrogate error rate time series generated from the non-EEG based model.

[Figure 6 about here.]

B. EEG-Based Error Rate Estimation

Multiple linear regression models and feedforward multi-layer networks were trained to estimate the behavioral error-rate time series from information available in the EEG power spectrum. Except where indicated, principal component analysis (PCA) was applied to the full EEG log spectrum to extract the directions of largest variance for each session used to train the network. Projections of the EEG log spectral data on the subspace formed by the eigenvectors corresponding to the largest eigenvalues were then used as input to train various models to estimate the time course of the local error rate. Each model was trained on one session and tested on a separate test session for each of the 10 subjects. PCA eigenvectors derived from the training session were used to preprocess data from the testing session, so that both training and test data were preprocessed in the same way. Mean and standard deviation of rms estimation errors between observed and estimated error rates were then computed for all 20 training-testing pairs for each network architecture.

B.1 Number of Principal Components

We first studied the effect of the number of principal components used on estimation performance of a linear regression model. We found that using four principal components (accounting for over 89% of the variance) provided the most effective estimate. Any further accuracy increase from using more principal factors was outweighed by the additional computational expense and noise introduced into the model. This result confirms a recent finding of Makeig and Jung [22] who showed significant correlations between the first four eigenvectors of EEG spectral variance and alertness on the same detection task. In further model comparisons, therefore, we used four principal components as input.

B.2 Advantage of Using the Full EEG Spectrum

Most studies relating task performance to the EEG spectrum have focused on a small number of EEG spectral bands defined *a priori*, rather than the full-spectrum. To determine the improvement, if any, in error-rate estimation using the full EEG spectrum, we compared the results of error-rate estimation using linear regression on the full log spectrum, reduced to four principal factors, with results of linear regression on EEG power at five frequencies previously shown to be correlated to error rate (3.1, 9.2, 13.4, 19.5, and 39 Hz) [9]. PCA-reduced full log spectra resulted in lower mean rms estimation error across 20 training-testing pairs (rms error 0.1633 versus 0.2008). Analysis of variance showed this difference to be highly significant across subjects ($F(1,9) = 197.9, p < 0.001$). Therefore, in further comparisons, we used the full EEG log spectrum as input, rather than a subset of pre-selected frequencies.

B.3 Advantage of Using Two EEG Channels

A previous investigation using a similar paradigm [9] applied linear regression models to the EEG power spectrum at single scalp channels to estimate alertness. In this study, we first compared the results of using log spectral data from two channels (Cz, and Pz/Oz) against results of using data from either channel alone. Table I shows that mean rms error across 20 training-testing pairs, as estimated by linear regression on PCA-reduced log spectra (0.6-24.4 Hz), is significantly lower using two data channels than using either Cz ($F(1,10) = 19.881; p = 0.001$) or Pz/Oz ($F(1,10) = 8.047; p = 0.018$)

alone. Therefore, for further comparisons we used EEG log power spectra from both scalp sites as input.

[Table 1 about here.]

B.4 Advantage of Using Neural Networks

Next, we compared the accuracy of linear regression against that of two-layer (no hidden layer) and three-layer (one hidden layer) neural networks. The number of hidden units in the three-layer network varied from 2 to 6. For each network architecture, the time course of error rate was estimated five times, using different random initial weights in the range [-0.3,0.3] for each of the 20 training-testing session pairs. Results of neural network estimation were then compared to those using linear regression models [9]. The nonlinear adaptability of multi-layer perceptrons significantly improved estimation performance over linear regression, reducing the rms error on the testing data across subjects ($F(1,9) = 6.370; p = 0.03$, Table II). The performance of three-layer nets was only slightly (and non-significantly) better than that of two-layer nets (F(1,9)=0.335, n.s.), suggesting that the major advantage afforded by the neural nets derived from their nonlinear squashing functions. In further testing, we chose to use three-layer networks with three hidden units.

[Table 2 about here.]

[Figure 7 about here.]

Figure 7 plots actual and estimated error rate time series for single test sessions from the two typical subjects. The error-rate estimates were obtained using both linear regression and three-layer neural networks with three hidden units applied to two-channel EEG log power spectra projected on the four principal components. As can be seen in the figure, in both sessions the neural networks estimate changes in local error rate occurring throughout the sessions reasonably well and with less estimation error than the linear regression estimates.

[Figure 8 about here.]

B.5 Performance of EEG-based Alertness Estimates

Finally, we compared the accuracy of our best EEG-based estimates to those produced by the *a priori* standards and the lower-bound for the same sessions. Figure 8 displays results for each session, sorted in increasing order of total rms error. The top panel shows that the estimation errors produced by both the more realistic ("group trend") and unrealistic ("right stuff") *a priori* models were larger than those produced by the EEG-based linear and nonlinear (3-layer neural network) models. EEG-based nonlinear estimators gave lower rms estimation error than the conservative "group trend" estimates for 18 of the 20 training-testing pairs, demonstrating that suitable EEG-based algorithms are capable of giving more accurate estimates of performance than even optimum *a priori* estimators. EEG-based estimators were also considerably more accurate than the predictions of the unrealistic "right stuff" model.

The bottom panel of Figure 8 shows the estimation errors expected from sampling error alone (mean$\pm$2 s.d.). As can be seen, rms estimation error is within two standard deviations of the expected lower bound for 13 of the 20 EEG-based session estimates. On average, EEG-based estimation errors were 1.2 standard deviations above the lower bound. These results suggest that continuous EEG-based error-rate estimation using a small number of data channels is feasible, and can give more accurate information about minute-to-minute changes in operator alertness than even the best *a priori* models.

V. DISCUSSION

Results of analysis of EEG and auditory detection data from 20 eyes-open experiments on 10 subjects confirm that continuous and accurate estimates of operators' levels of alertness, as indexed by a local

error rate measure, can be derived from EEG data collected at two (central and posterior midline) scalp sites. The computational load imposed by our full-spectrum analysis is well within the capabilities of modern digital signal processing hardware to perform in real time using one or more channels of EEG data. Once an estimator has been developed for each operator, based on limited pilot testing, the method uses only spontaneous EEG signals from the operator, and does not require further collection or analysis of operator performance. Also, unlike proposed methods based on event-related potentials [23], [24], [25], our method avoids introducing potentially distracting probe or secondary-task stimuli into the operator's environment.

Several important issues remain to be resolved before practical alertness monitoring systems can be implemented. These include: (1) Determing to what extent an index of alertness based on auditory detection performance predicts fluctuations in performance on other tasks; (2) Minimizing the amount and quality of pilot training data required from individual subjects; (3) Separating muscle and eye movement data from the EEG records, and using these to further improve the accuracy and reliability of the estimation; (4) Developing methods for real-time data normalization, instead of normalizing each session separately; (5) Determining optimum recording locations; and (6) Developing and testing portable and convenient electrode technology. If these issues can be resolved satisfactorily, the methods described in this paper may have important practical applications to research and operational environments in which near real-time knowledge of changes in operator alertness may be useful or critical.

VI. CONCLUSION

Sorting power spectra by local error rate, and correlating changes in EEG power with changes in error rate demonstrate a monotonic relationship between minute-scale changes in performance and the EEG spectrum. This relationship appears stable within individuals across sessions, but is somewhat variable between subjects. We have investigated the feasibility of practical alertness monitoring by combining power spectrum estimation, principal component analysis, and artificial neural networks. Our results show that accurate, individualized alertness estimation using neural networks applied to EEG spectral data appears realistic. Results of neural network estimation using the full EEG spectrum compare favorably to previous results using a linear regression model applied to EEG power at preselected frequencies [9]. The practical potential of EEG-based alertness estimation is suggested by the relative accuracy of EEG-based estimates compared to those of the best *a priori* models.

References

[1] N. Mackworth, "The breakdown of vigilance during prolonged visual search.," *Quart. J. Exp. Psychol.*, vol. 1, pp. 6–21, 1948.

[2] H. Davis, P. Davis, A. Loomis, E. Harvey, and G. Hobart, "Human brain potentials during the onset of sleep.," *J. Neurophysiol.*, vol. 1, pp. 24–38, 1938.

[3] H. Williams, A. Granda, R. Jones, A. Lubin, and J. Armington, "EEG frequency and finger pulse volume as predictors of reaction time during sleep loss," *Electroencephalogr. Clin. Neurophysiol.*, vol. 14, pp. 64–70, 1962.

[4] H. Fruhstorfer and R. Bergstrom, "Human vigilance and auditory evoked responses.," *Electroencephalogr. Clin. Neurophysiol.*, vol. 27, no. 4, pp. 346–355, 1969.

[5] J. Santamaria and K. Chiappa, "The EEG of drowsiness in normal adults.," *J. Clinical Neurophysiology.*, vol. 4, no. 4, pp. 327–382, 1987.

[6] J. Stroud, "The fine structure of psychological time.," *Annals of the New York Academy of Sciences*, vol. 138, no. 2, pp. 623–631, 1967.

[7] J. Stebel and R. Sinz, "On central nervous minute-periodicity and its coordination.," *J. Interdisc. Cycle Res.*, vol. 2, pp. 63–72, 1971.

[8] M. Treisman, "Temporal rhythms and cerebral rhythms," in *Timing and Time Perception* (J. Gibbon and L. Allan, eds.), vol. 423, pp. 542–565, NY Acad. Sci., 1984.

[9] S. Makeig and M. Inlow, "Lapses in alertness: coherence of fluctuations in performance and EEG spectrum.," *Electroencephalogr. Clin. Neurophysiol.*, vol. 86, pp. 23–35, 1993.

[10] J. Beatty, A. Greenberg, W. P. Deibler, and J. O'Hanlon, "Operant control of occipital theta rhythm affects performance in a radar monitoring task.," *Science*, vol. 183, pp. 871–873, 1974.

[11] M. Matoušek and I. Petersén, "A method for assessing alertness fluctuations from EEG spectra.," *Electroencephalogr. Clin. Neurophysiol.*, vol. 55, no. 1, pp. 108–113, 1983.

[12] A. Belyavin and N. Wright, "Changes in electrical activity of the brain with vigilance.," *Electroencephalogr. Clin. Neurophysiol.*, vol. 66, no. 2, pp. 137–144, 1987.

[13] R. Venturini, W. Lytton, and T. Sejnowski, "Neural network analysis of eevent related potentials and electroencephalogram.," in *Advances in Neural Information Processing Systems* (J. E. Moody, S. J. Hanson, and R. P. Lippmann, eds.), vol. 4, pp. 651–658, Morgan Kaufmann, 1992.

[14] S. Makeig, F. Elliott, and M. Postal, "First demonstration of an alertness monitoring/management system," Tech. Rep. 93-36, Naval Health Research Center, San Diego, CA, 1993.

[15] M. Steriade, "Central core modulation of spontaneous oscillations and sensory transmission in thalamocortical systems," *Current Opinion in Neurobiology*, vol. 3(4), pp. 619–25, 1993.

[16] P. Sneath and R. Sokal, *Numerical taxonomy: the principles and practice of numerical classification*. San Francisco: W. H. Freeman, 1973.

[17] G. Perlman, "UNIX/STAT: Data-analysis programs," *Behavior Research Methods and Instrumentation*, no. 1, 1984.

[18] D. van Camp, *User's guide for the Xerion neural network simulator*. Department of Computer Science, University of Toronto, 1993.

[19] D. E. Rumelhart, G. E. Hinton, and R. J. Williams, "Learning internal representation by error propagation," *in: Rummelhardt "Parallel distributed processing", Chap. 8*, 1986.

[20] N. Morgan and H. Bourlard, "Generalization and parameter estimation in feedforward nets: some experiments," in *Advances in Neural Information Processing Systems* (D. S. Touretzky, ed.), vol. 2, pp. 630–637, Morgan Kaufmann Publishers, 1990.

[21] A. Papoulis, "Minimum bias windows for high resolution spectral estimation," *IEEE Transactions on Information Theory*, vol. IT-19, pp. 9–12, 1973.

[22] S. Makeig and T. Jung, "Alertness is a principal component of variance in the EEG spectrum," *NeuroReport*, vol. 7, no. 1, pp. 213–216, 1995.

[23] S. Makeig, F. Elliott, M. Inlow, and D. Kobus, "Lapses in alertness: Brain-evoked responses to task-irrelevant auditory probes," Tech. Rep. 90-39, Naval Health Research Center, San Diego, CA, 1992.

[24] S. Hillyard and P. Johnston, "Event-related brain potentials as predictors of target detection performance in a moving waterfall display simulating passive broad-band sonar monitoring," Tech. Rep. 93-33, Naval Health Research Center, San Diego, CA, 1994.

[25] J. Isreal, C. Wickens, G. Chesney, and E. Donchin, "The event-related brain potential as an index of display-monitoring workload," *Human Factors*, vol. 22(n2), pp. 211–224, 1980.

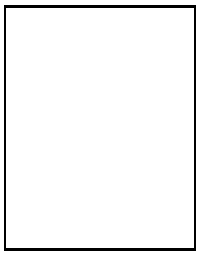

Tzyy-Ping Jung received the B.S. degree in Electronics Engineering from National Chiao Tung University, Taiwan in 1984, and received his M.S. and Ph.D. degrees in Electrical Engineering from The Ohio State University in 1989 and 1993, respectively. He is currently a Research Associate at the National Research Council of the National Academy of Sciences. He is also a Research Associate with the Computational Neurobiology Laboratory at The Salk Institute in San Diego, CA. His research interests are in the areas of speech production and perception, signal processing, artificial neural networks, time-frequency analysis of human EEG, and the development of neural human-system interfaces.

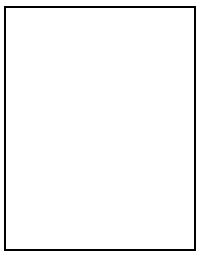

Scott Makeig is a psyhobiologist specializing in applying time-frequency and neural network analysis to human EEG and fMRI time-series data. He received a B.A. from UC Berkeley in 1972, completed a Master's degree program in Music Theory from the University of South Carolina in 1979, and received an interdisplinary Ph.D. from the University of California San Diego in 1982 entitled "Music Psychobiology." Dr. Makeig is on the faculty of the Department of Neurosciences at UCSD, and for several years has studied the EEG correlates of alertness lapses for the Office of Naval Research as a research psychologist at the Naval Health Research Center, San Diego.

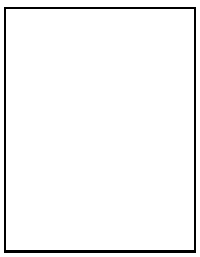

Magnus Stensmo received an MSc in Computer Science and Engineering and a PhD in Computer Science from the Royal Institute of Technology in Stockholm, Sweden. He is now a postdoctoral research associate with the Computer Science Division at University of California, Berkeley.

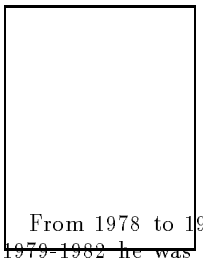

Terrence J. Sejnowski is an Investigator with the Howard Hughes Medical Institute and a Professor at The Salk Institute for Biological Studies where he directs the Computational Neurobiology Laboratory. He is also Professor of Biology and Adjunct Professor in the Departments of Physics, Neuroscience, Psychology, Cognitive Science, Electrical and Computer Engineering, and Computer Science and Engineering at the University of California, San Diego, where he is Director of the Institute for Neural Computation and Director of the McDonnell-Pew Center for Cognitive Neuroscience. Dr. Sejnowski received B.S. in physics from the Case-Western Reserve University, M.A. in physics from Princeton University, and a Ph.D. in physics from Princeton University in 1978.

From 1978 to 1979 Dr. Sejnowski was a postdoctoral fellow in the Department of Biology at Princeton University and from 1979-1982 he was a postdoctoral fellow in the Department of Neurobiology at Harvard Medical School. In 1982 he joined the faculty of the Department of Biophysics at the Johns Hopkins University, where he achieved the rank of Professor before moving to San Diego in 1988.

Dr. Sejnowski received a Presidential Young Investigator Award in 1984. He was a Wiersma Visiting Professor of Neurobiology at the California Institute of Technology in 1987. In 1988 he founded the journal Neural Computation, published by the MIT Press. He delivered the 1991 Messenger Lectures at Cornell University. With Patricia Churchland, he wrote "The Computational Brain", published by the MIT Press in 1992. He was a Sherman Fairchild Distinguished Scholar at the California Institute of Technology in 1993-1994 and continues as a Visiting Professor.

The long-range goal Dr. Sejnowski's research is to build linking principles from brain to behavior using computational models. This goal is being pursued with a combination of theoretical and experimental approaches at several levels of investigation ranging from the biophysical level to the systems level. Hippocampal and cortical slice preparations are being used to explore the properties of single neurons. Network models based on these data are used to study how populations of neurons code and process information. These studies may lead to new insights into how sensory information is represented in the visual cortex, how memory representations are formed, and how sensorimotor transformations are organized.

List of Figures

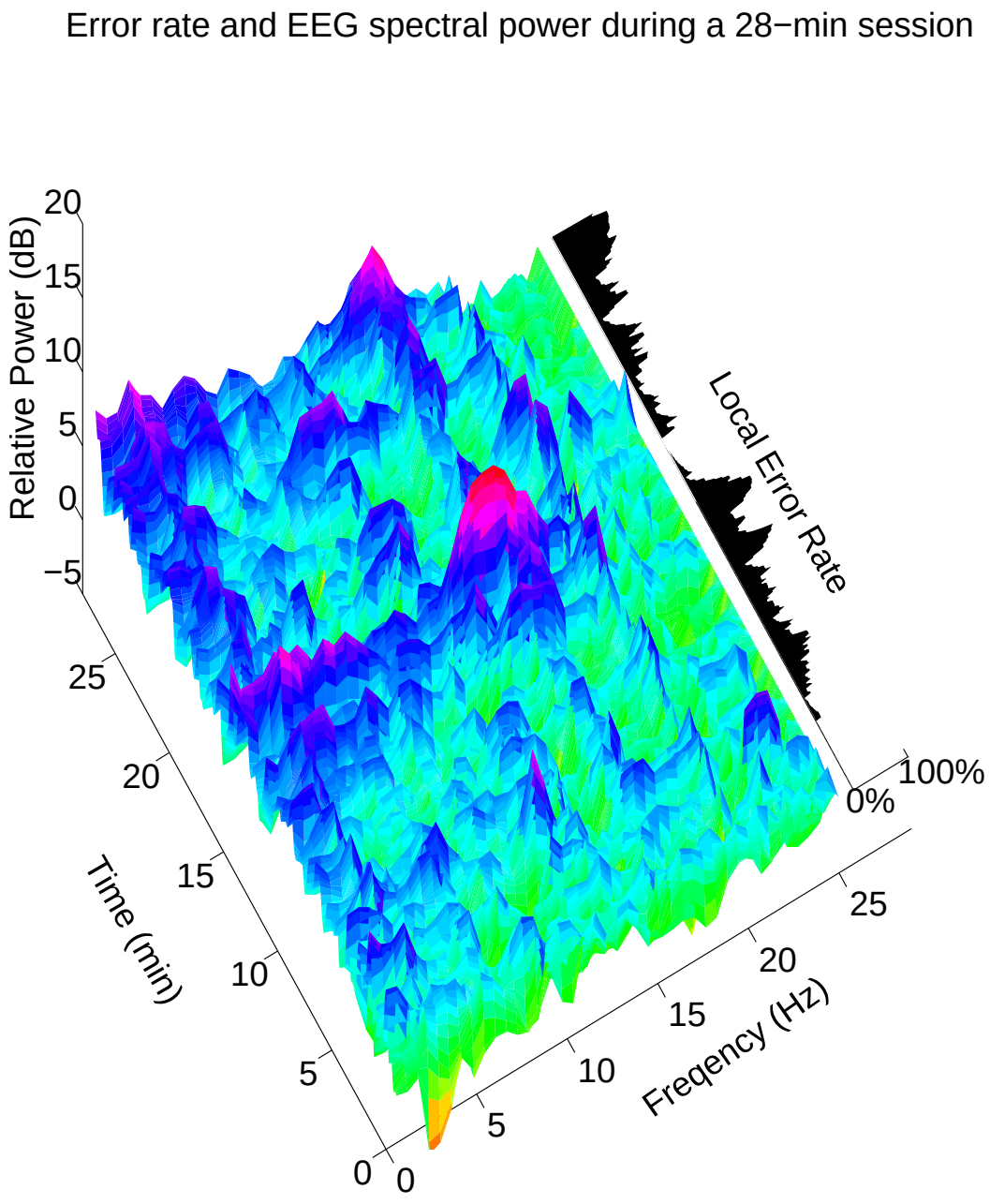

Fig. 1. Fluctuations in *local error rate* and in EEG log power (at site Cz) during one test session. Note the correlations between periods of high local error rate and increased spectral power, particularly near 4 Hz and near 14 Hz. Here, the local error rate is the percentage of (10/min) targets not responded to in a moving 33-s exponential window. EEG has been smoothed using the same window and normalized by subtracting the log mean power spectrum during the first two minutes of error-free performance from each log spectral trace. Subject: D3 (cf. Fig. 3c).

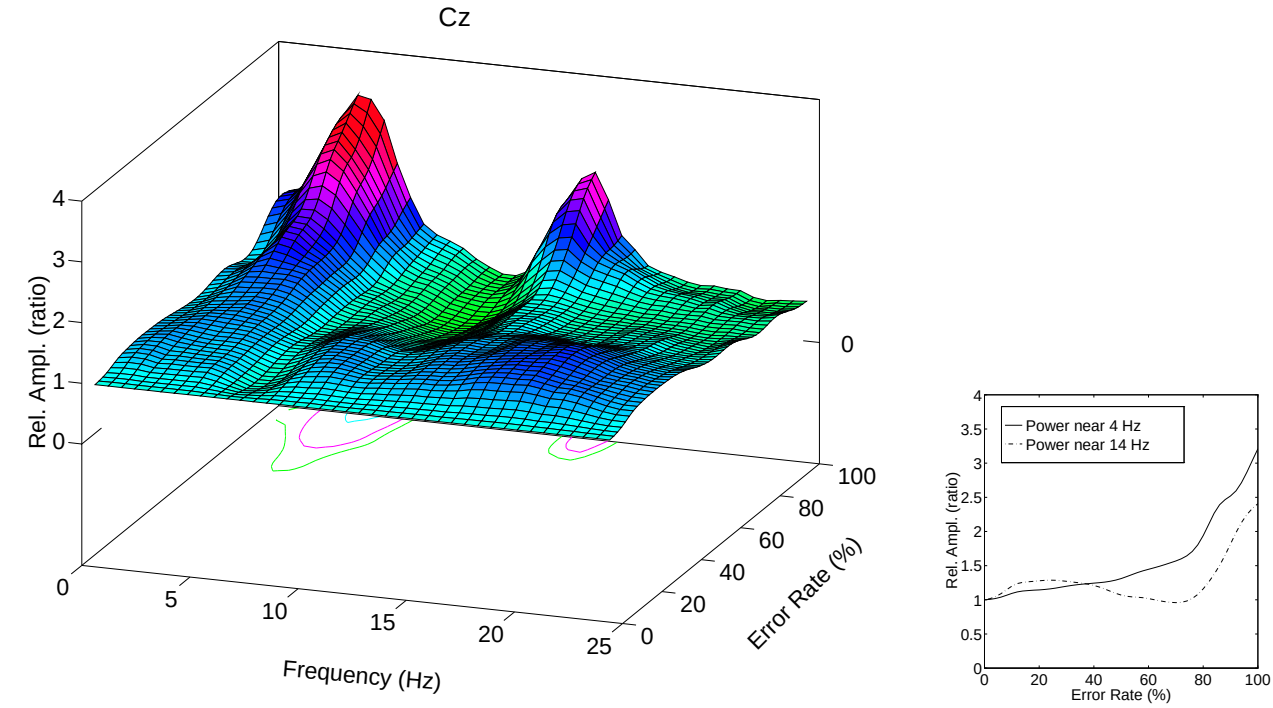

(a)

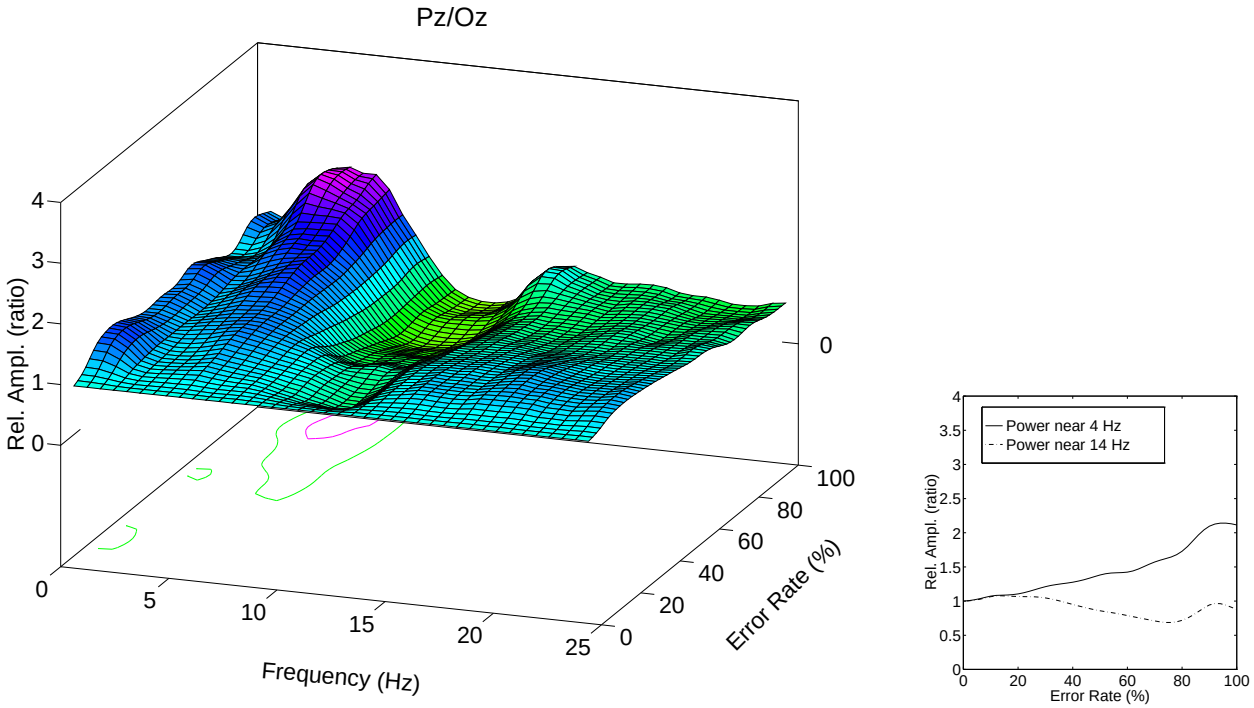

(b)

Fig. 2. Grand mean *error-sorted spectra* showing mean group differences between drowsy and alert log spectra for each local error rate level (indexing levels of drowsiness). Grand mean of 20 sessions from 10 subjects. Error rate smoothing in this and following figures: causal 93-s exponential window. (a) At the vertex (Cz), spectral changes are largest near 4 Hz and 14 Hz at high error rates. (Insert shows cross-sections of power change with error rate at those frequencies). (b) At Pz/Oz (midway between midline parietal and occipital sites), power increases near 4 Hz beginning at moderate error rates, and decreases slightly near 10 Hz. (Insert, as in part (a)).

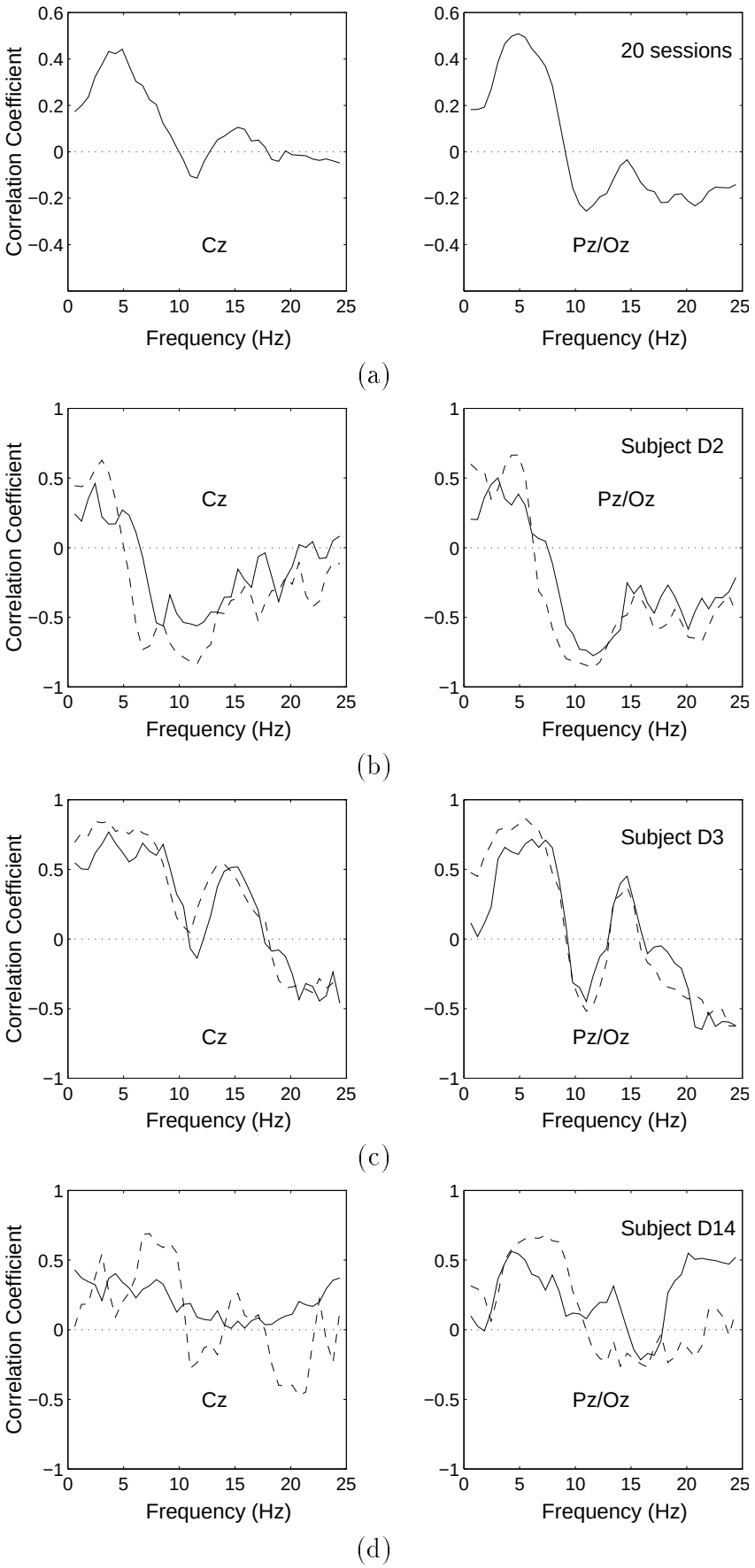

Fig. 3. *Correlation spectra.* Correlations between EEG log power and local error rate, computed separately for 40 EEG frequencies between 0.6 and 24.4 Hz. (a) Grand mean correlation spectra for 20 sessions on 10 subjects. (b)(c) Comparisons of pairs of sessions from two typical subjects, D2 and D3 (cf. Fig. 1). (d) Correlation spectra from the least similar within-subject session pair (subject D14).

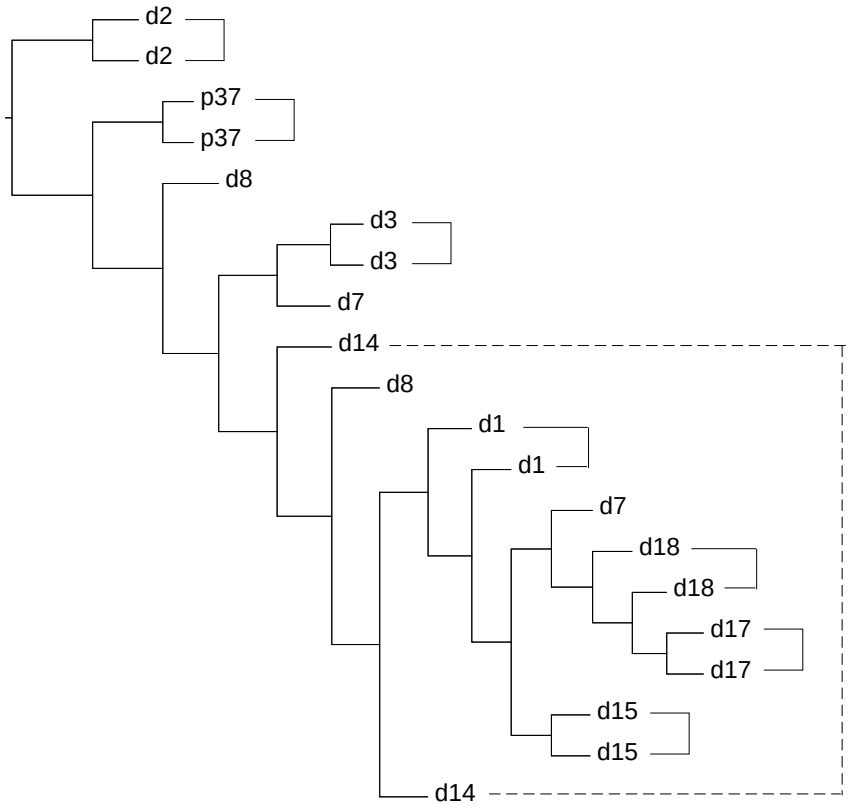

Fig. 4. Within-subject reproducibility of EEG changes accompanying loss of alertness. Hierarchical cluster analysis of correlation spectra composed of correlations between changes in the EEG log spectrum and detection performance at 40 EEG frequencies for two sessions each from 10 subjects. Note that for most subjects, within-subject session pairs are grouped together (solid lines on right). Correlation spectra for two typical subjects (D2 and D3), and for the subject whose sessions were the most widely separated by the analysis (D14, dashed line) are shown in Fig. 3.

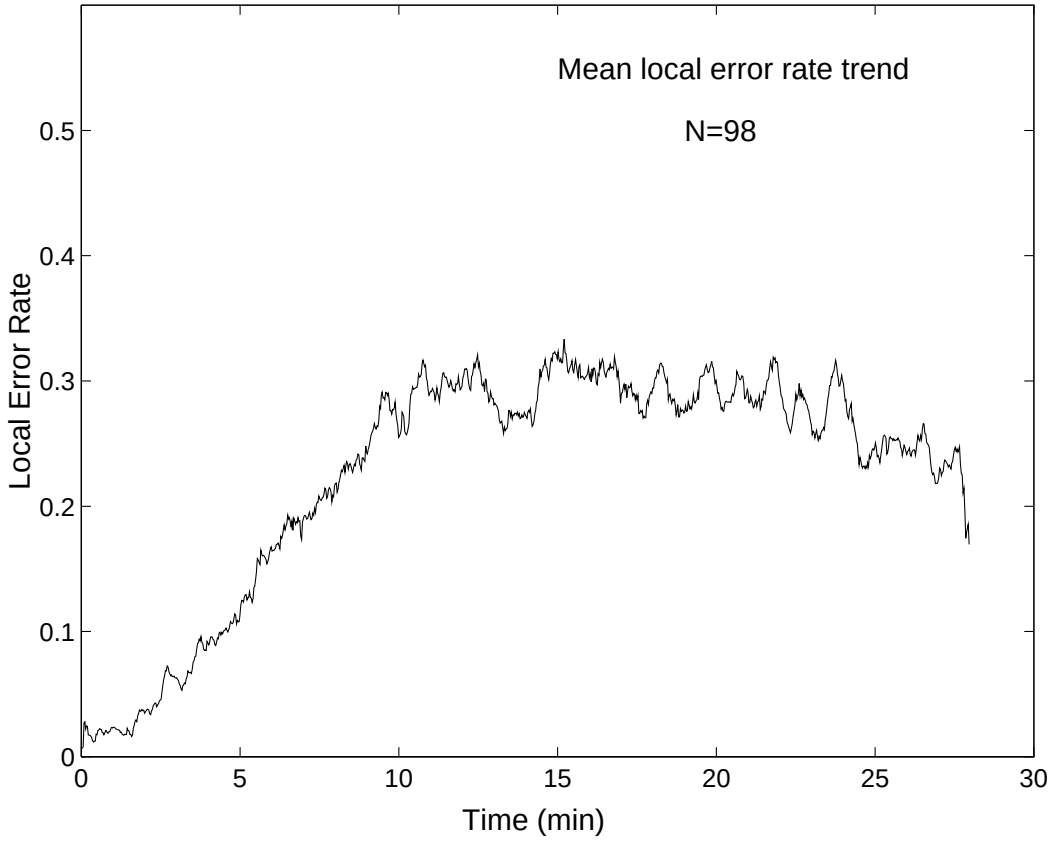

Fig. 5. Group mean local error rate trend for each time-on-task, averaged across 98 sessions. This group mean trend gives a conservative *a priori* standard of comparison for EEG-based estimation errors in the auditory detection task.

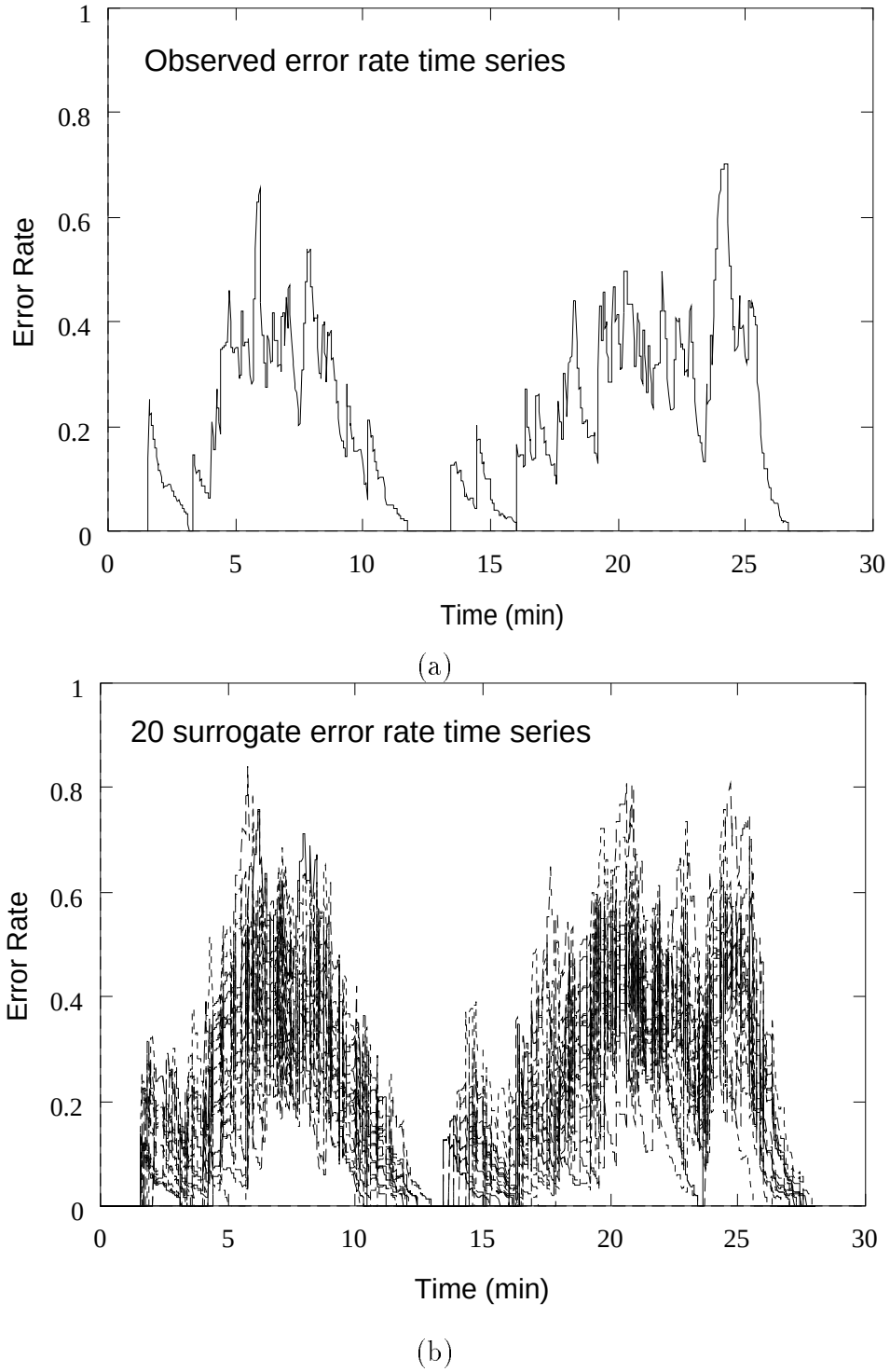

Fig. 6. Illustration of the method used to generate a lower bound for estimation error in each session. (a) An observed local error rate time series, and, (b) 20 surrogate error rate time series for the same session, generated by random during the first two minutes of error-free performance from each log spectral trace. Subject: D3 (cf. Fig. 3c).

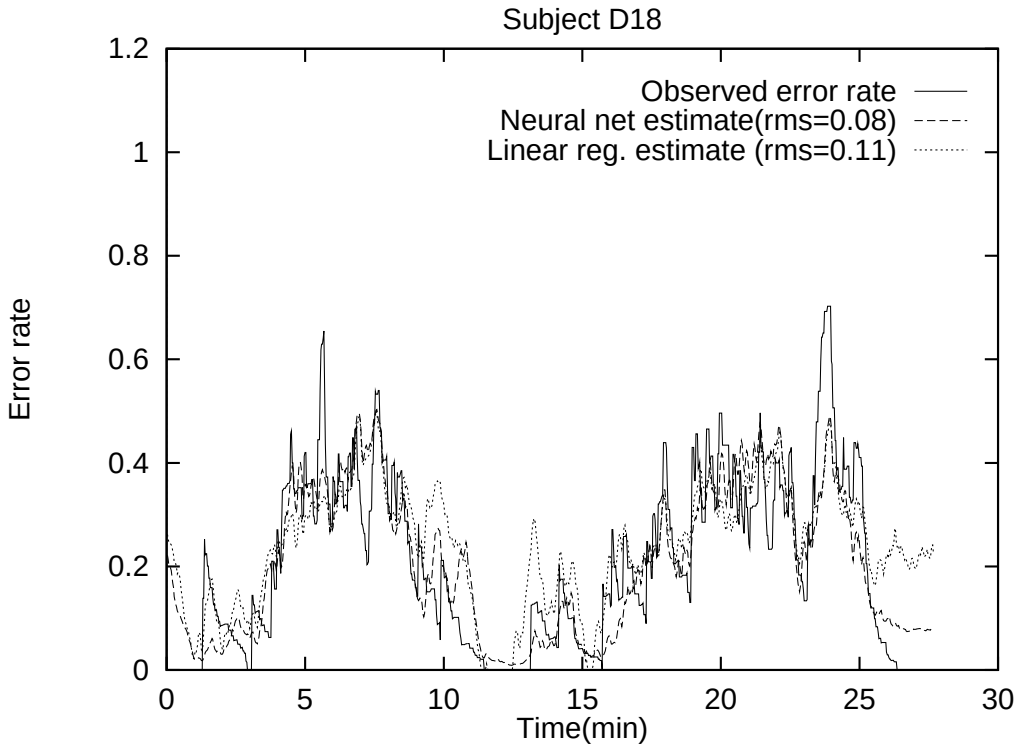

(a)

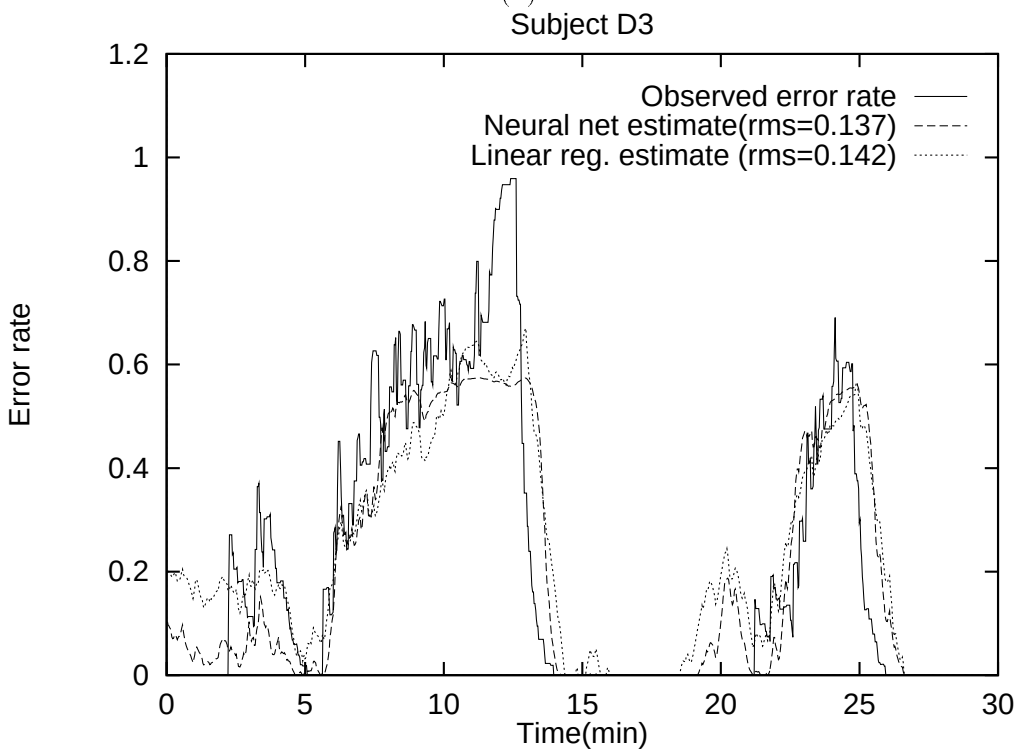

(b)

Fig. 7. Error-rate estimates for sessions from two subjects, based on 3-layer feedforward neural network (dashed lines) and [0,1]-limited linear regression (dotted lines) processing of PCA-reduced EEG log spectra at two scalp sites, overplotted against actual local error rate time series for the sessions (solid lines). For both sessions, the nonlinear estimator gives the lower root mean-square (rms) estimation error. Note differences at the end of (a) and beginning of (b).

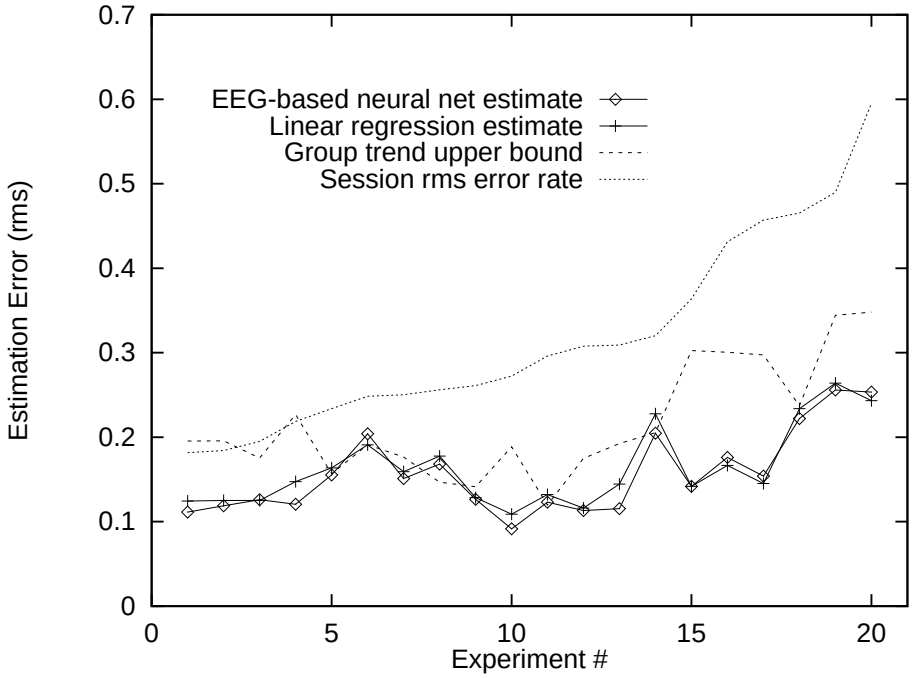

(a)

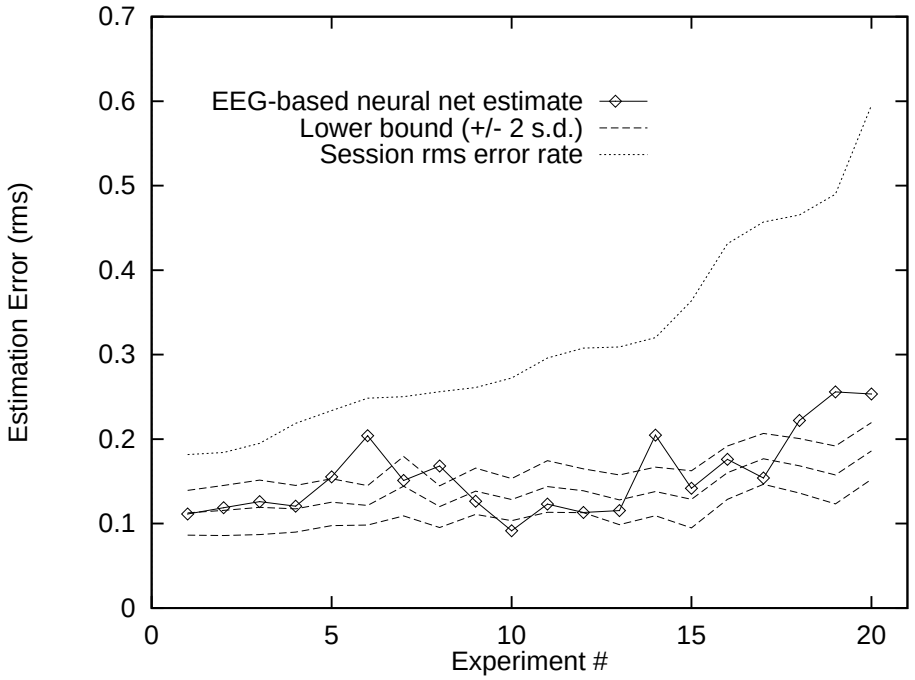

(b)

Fig. 8. Relative accuracy of EEG-based versus best *a priori* local error-rate estimators. (a) Estimation errors produced by EEG-based linear-regression and 3-layer neural network models (see key) compared to errors produced by optimum (observed group trend) and unrealistic (zero-error) *a priori* models. Neural network models give a lower estimation error than linear-regression models in 16 of 20 cases ($F(1,9) = 6.37; p = 0.03$), and a lower estimation error than the optimum *a priori* models in 18 of 20 cases. (b) EEG-based rms estimation error compared to an expected lower bound for estimation error (mean +/- 2 s. d.) computed for each session using a Monte Carlo method (see Fig. 6).

List of Tables

TABLE I

COMPARISON OF MEAN ESTIMATION ERRORS IN ERROR-RATE ESTIMATES USING MULTIPLE LINEAR REGRESSION APPLIED TO EEG POWER AT FIVE FREQUENCIES FROM TWO EEG CHANNELS. AVERAGES OF 20 SESSIONS ON 10 SUBJECTS. A REGRESSION MODEL FOR EACH SESSION WAS USED TO ESTIMATE THE TIME COURSE OF THE ERROR RATE IN A SECOND SESSION FROM THE SAME SUBJECT.

Measure	*EEG site*		
	Cz	Pz/Oz	Cz+Pz/Oz
rms est. error	0.1785	0.1919	0.1633
std. deviation	0.0452	0.0684	0.0458

TABLE II

COMPARISON OF MEAN ESTIMATION ERRORS IN ERROR-RATE ESTIMATES USING MULTIPLE LINEAR REGRESSION AND NEURAL NETWORKS. FOR EACH SUBJECT, THE FULL EEG SPECTRUM FROM ONE SESSION, PREPROCESSED USING PRINCIPAL COMPONENT ANALYSIS (PCA), WAS USED TO TRAIN THE MODELS TO ESTIMATE THE TIME COURSE OF ERROR RATE IN A SECOND SESSION FROM THE SAME SUBJECT. THE TABLE SHOWS THE MEANS AND STANDARD DEVIATIONS OF THE ROOT MEAN SQUARE (RMS) ESTIMATION ERROR FOR 20 SESSIONS FROM 10 SUBJECTS.

Measure	*Estimate*		
	Linear Regression	Neural Network (no hidden layer)	Neural Network (1 hidden layer with 3 units)
rms est. error	0.163	0.158	0.156
std. deviation	0.0452	0.0429	0.0475